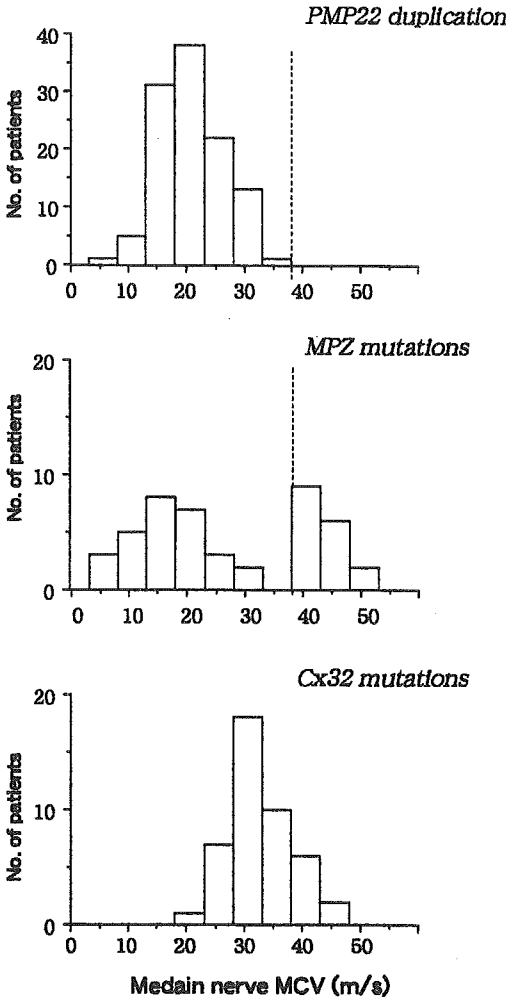

Fig. 2 Frequency distribution of median nerve MCVs in CMT patients with PMP22 duplication, MPZ mutations and Cx32 mutations.

was also more frequent in the axonal subgroup. Other motor and sensory symptoms did not differ significantly between the two subgroups (Table 1). These associated symptoms were seen in association with several types of MPZ mutations.

Pathology of the sural nerve

In PMP22 duplication, myelinated fibre density was variably reduced, ranging from 183 to 6854/mm^2 (Table 3, Fig. 3). Unmyelinated fibre density was also variably reduced but relatively preserved, ranging from 16 157 to 28 160/mm^2. Fibres showing demyelinating pathology in teased-fibre preparations represented 80.1 ± 17.7% of the total, while axonal pathology was seen in 0.7 ± 2.8%. Tomacula and globule formation in teased fibres was variable among patients, with a mean frequency of 7.3 ± 6.5% of fibres (Fig. 4). Onion bulbs were present to varying degrees, ranging from 10 to 83% of myelinated fibres, appearing in half of the myelinated fibres and showing a mean of 3.94 lamellae (Table 3, Fig. 3). Axonal sprouts were generally rare, but in some patients axonal sprouts were abundant (Table 3, Fig. 3). These findings indicate that in PMP22 duplication demyelinating pathology was predominant, while axonal loss and axonal sprouts were variably present.

In MPZ mutations, myelinated and unmyelinated fibre densities were also variable, ranging from 510 to 8279/mm^2 and 10 387 to 36 874/mm^2, respectively (Table 3). The frequency of demyelinating and axonal pathology was significantly variable among individual patients. When patients were subdivided into those with median nerve MCV ≤38 m/s (demyelinating) and those with higher MCV (axonal), myelinated fibre densities were significantly lower in the demyelinating subgroup than in the axonal subgroup ($P < 0.05$; Table 3), while unmyelinated fibre density did not differ significantly between subgroups (Table 3, Fig. 3). The frequencies of fibres with demyelinating pathology, tomacula and globule formation, and onion bulbs were significantly greater in the demyelinating subgroup ($P < 0.0001$, $P < 0.001$ and $P < 0.05$, respectively). An uncompacted myelin sheath was occasionally observed. In contrast, the frequency of fibres with axonal pathology and the density of axonal sprouts were significantly greater in the axonal subgroup ($P < 0.01$ and $P < 0.05$, respectively; Table 3, Fig. 4). In individual patients with MPZ mutations, pathological features in which either demyelinating or axonal involvement was predominant, combined or concomitant demyelinating and axonal pathological findings were rare. Thus, pathological features were distinctive between the demyelinating and axonal subgroups defined by median nerve MCV.

In Cx32 mutations, myelinated fibre density was diminished, but less markedly than in PMP22 duplications and MPZ mutations (Table 3). Unmyelinated fibres were also relatively well preserved (Table 3). Less marked reduction in the myelinated and unmyelinated fibre density reflected the frequent presence of axonal sprouts (Table 3, Fig. 3). Teased-fibre preparations showed fibres with demyelinating and axonal pathologies, but both were mild. Globule and tomacula formation and onion bulb formation were also mild (Table 3, Fig. 4). However, axonal sprouts were frequent, ranging from 340 to 2610/mm^2 (Table 3). Large myelinated axon loss and axonal sprouts were variable among the patients. Axonal and demyelinating pathologies were invariably present in combination in individual patients, although axonal features were predominant.

Median nerve MCVs, CMAPs and sural nerve pathology in relation to disease advancement

In PMP22 duplication, slowed median MCV (≤38 m/s) was seen for all ages at examination (Fig. 5A) and durations of illness (data not shown). Median nerve CMAPs tended to decrease with advancing age ($r = 0.28$, $P < 0.013$; Fig. 5A) and with disease duration (not significant; data not shown). In Cx32 mutations, moderately slowed MCV (22.8–46.6 m/s)

Table 3 *Pathological features of sural nerves in 44 CMT patients*

Mutations	Myelinated fibre density (no./mm²)	Unmyelinated fibre density (no./mm²)	Teased-fibre study		
			De-/remyelination (%)	Axonal (%)	Globule/tomacula (%)
PMP22 duplication (n = 23)	2612 ± 2348 (183–6854)	20 196 ± 5658 (16 157–28 160)	80.1 ± 17.7 (39–100)	0.7 ± 2.8 (0–3.5)	7.3 ± 6.5 (0–18)
MPZ mutations (n = 11)	2208 ± 1864 (501–8279)	22 197 ± 8452 (10 387–36 874)	65.6 ± 39.2 (5–94)	1.9 ± 2.1 (0–5)	3.9 ± 2.6 (0–7)
MCV ≤38 m/s (n = 6)	1146 ± 646	18 742 ± 7487	85.0 ± 18.7	1.2 ± 1.8	5.4 ± 4.0
MCV >38 m/s (n = 5)	4631 ± 844	26 515 ± 8426	7.5 ± 3.5	4.0 ± 1.4	0.3 ± 0.9
	*	NS	***	**	**
Cx32 mutations (n = 10)	6090 ± 1158 (4176–12 711)	34 705 ± 9053 (25 165–43 175)	9.2 ± 6.4 (1–18)	4.2 ± 2.4 (1–7)	3.0 ± 2.3 (0–4)
Controls (n = 9)	8190 ± 511	29 913 ± 3457	3.8 ± 2.2	0.5 ± 0.8	0

Mutations	Onion bulbs		Axonal sprouts (no./mm²)	G ratio
	Rate (no./MFD)	Lamellae (no./mm²)		
PMP22 duplication (n = 23)	0.47 ± 0.29 (0.10–0.83)	3.94 ± 1.46 (1–6)	160 ± 210 (10–1085)	0.68 ± 0.05 (0.59–0.79)
MPZ mutations (n = 11)	0.22 ± 0.23 (0.03–0.80)	2.31 ± 1.20 (1–4)	350 ± 410 (0–1190)	0.71 ± 0.04 (0.64–0.76)
MCV ≤38 m/s (n = 6)	0.36 ± 0.22	2.97 ± 0.35	30 ± 20	0.70 ± 0.04
MCV >38 m/s (n = 5)	0.05 ± 0.07	1.00 ± 0.00	730 ± 290	0.74 ± 0.02
	*	*	*	NS
Cx32 mutations (n = 10)	0.06 ± 0.04 (0.04–0.14)	2.39 ± 0.26 (2–3)	1090 ± 830 (340–2610)	0.70 ± 0.05 (0.63–0.75)
Controls (n = 9)	0	–	<20	0.6–0.7

Data are mean ± standard deviation. Ranges are shown in parentheses. Control values are those described previously (Sobue, *et al.* 1989). *P < 0.01; **P < 0.001; ***P < 0.0001; NS = not significant.

was noted consistently for all ages at examination (Fig. 5A) as well as disease durations (data not shown). Median nerve CMAPs decreased with age (r = 0.45, P < 0.0013; Fig. 5A), and tended to decrease with duration of illness (not significant; data not shown). In MPZ mutations, however, two subgroups of MCVs were consistently present through all ages at examination (Fig. 5A) and durations of illness (data not shown). No tendency for CMAPs to decrease with advancing age or disease duration was observed (Fig. 5A).

Sural nerve pathology also changed markedly with disease advancement (Fig. 5B). In the PMP22 duplication, myelinated fibre density, in particular that of large myelinated fibres, decreased significantly with increasing age at examination (r = 0.71, P < 0.0001; Fig. 5B) and duration of illness (r = 0.40, P < 0.001; data not shown). Onion bulbs were rare in young patients, but their frequency increased with advancing age (r = 0.42, P < 0.01; Fig. 5B). In Cx32 mutations, large myelinated fibre density was relatively preserved in the younger patients, but decreased markedly with advancing age (r = 0.81, P < 0.001; Fig. 5B) and duration of illness (r = 0.37, P < 0.05; data not shown). Axonal sprouts were more frequent in older patients, and the density of axonal sprouts correlated well with age at examination (r = 0.68, P < 0.01; Fig. 5B) and duration of illness (r = 0.43, P < 0.01; data not shown). In cases with MPZ mutations, two small but distinctive subgroups were present, and were difficult to assess.

The MCV slowing was consistently preserved in spite of pathological changes in sural nerves in patients with PMP22 duplication and Cx32 mutations (Fig. 6). Median nerve MCVs were consistently slowed independently of large myelinated fibre loss, degree of onion bulb formation and axonal sprouts in the sural nerves (Fig. 6).

The findings indicate that MCVs in these three main genetic groups are consistently preserved independently of age at examination and disease duration; in patients with PMP22 duplication and Cx32 mutations, slowed MCVs are consistently preserved independently of the development of pathological changes. In contrast, CMAPs and large myelinated fibre populations tended to decrease with advancing age and disease duration. In cases with MPZ mutations, two relatively small but distinct subgroups with different MCVs were present, and tendencies related to age, disease duration and pathology were difficult to assess.

Concordance and discordance in MCVs among siblings, and gene mutations

In PMP22 duplication, all patients showed MCVs ≤38 m/s, though the extent of MCV reduction was variable. MCVs of

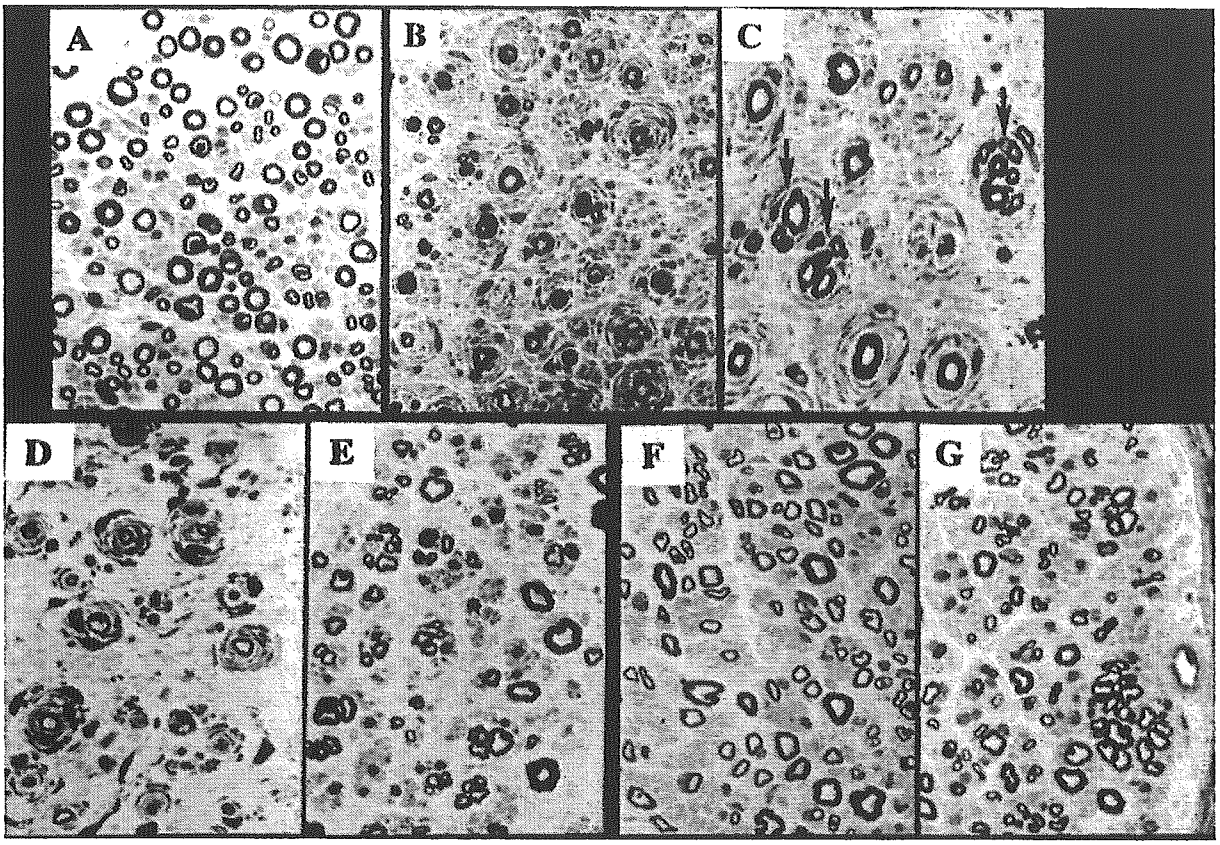

Fig. 3 (A) Transverse sections of the sural nerves from CMT patients. Myelinated fibre density was relatively well preserved but onion bulbs were rare in a 2-year-old patient with PMP22 duplication. (B) Myelinated fibre density was markedly decreased and onion bulb formation was prominent in a 43-year-old patient with PMP22 duplication. (C) Axonal sprouts were present at moderately density (arrows) in another patient with PMP22 duplication. (D and E) Onion bulb formation was prominent (D) in a patient with an MPZ mutation (Arg98His), while axonal sprouts were abundant (E) in another patient with an MPZ mutation (Thr124Met). Large myelinated fibres were significantly diminished in both of these patients. (F and G) Large myelinated fibre density was fairly well preserved in 16-year-old patient with a Cx32 mutation (Ser26Leu) (F), while they were markedly diminished and axonal sprouts were abundant (G) in a 61-year-old patient with a Cx32 mutation (Phe69Leu). Magnification: A, ×500; B, ×300; C, ×600; D–G, ×300.

≤38 m/s were seen concordantly among siblings in the 18 families in whom MCV was examined systemically (Table 4).

In MPZ mutations, probands with MCV ≤38 m/s in the median nerve (demyelinating subgroup) showed good concordance, with MCVs ≤38 m/s among siblings in the four families examined. Probands showing a median nerve MCV >38 m/s (axonal subgroup) exhibited good concordance, with MCV >38 m/s being noted among siblings in the four families (Table 4). The nature and position of amino acid substitutions in the MPZ protein were distinctly different among subgroups of patients with demyelinating and axonal phenotypes (Table 4), suggesting that demyelinating and axonal phenotypes in MCV are concordant in the siblings and are closely related to the nature and position of the amino acid substitution in MPZ.

In Cx32 mutations, the probands showed variable median nerve MCVs, including values more and less than 38 m/s. MCVs were discordant in terms of the 38 m/s cut-off value among siblings in the six families examined (Table 4). MCVs in these families were concordant among siblings in showing a range from 22.8 to 46.6 m/s. Thus, in most of the families, median nerve MCVs were discordant at the division point of 38 m/s but were concordant when the MCV range was set between 22.8 and 46.6 m/s (Table 4).

Muscle wasting, CMAPs and MCVs

Muscle weakness and atrophy were most pronounced in the distal portion of the leg and were noted to a lesser extent distally in the upper limbs; proximal muscles were only minimally involved. This distal and lower-limb-predominant motor involvement was common to all three main types of gene abnormality (Table 5). Table 6 shows the correlation between CMAPs and the strength of distal limb muscles in patients with PMP22 duplication, MPZ mutations and Cx32 mutations. The amplitude of CMAPs of median, ulnar and tibial nerves correlated significantly with corresponding distal muscle strengths ($r = 0.35$–0.69, $P < 0.05$–0.0005; Table 5).

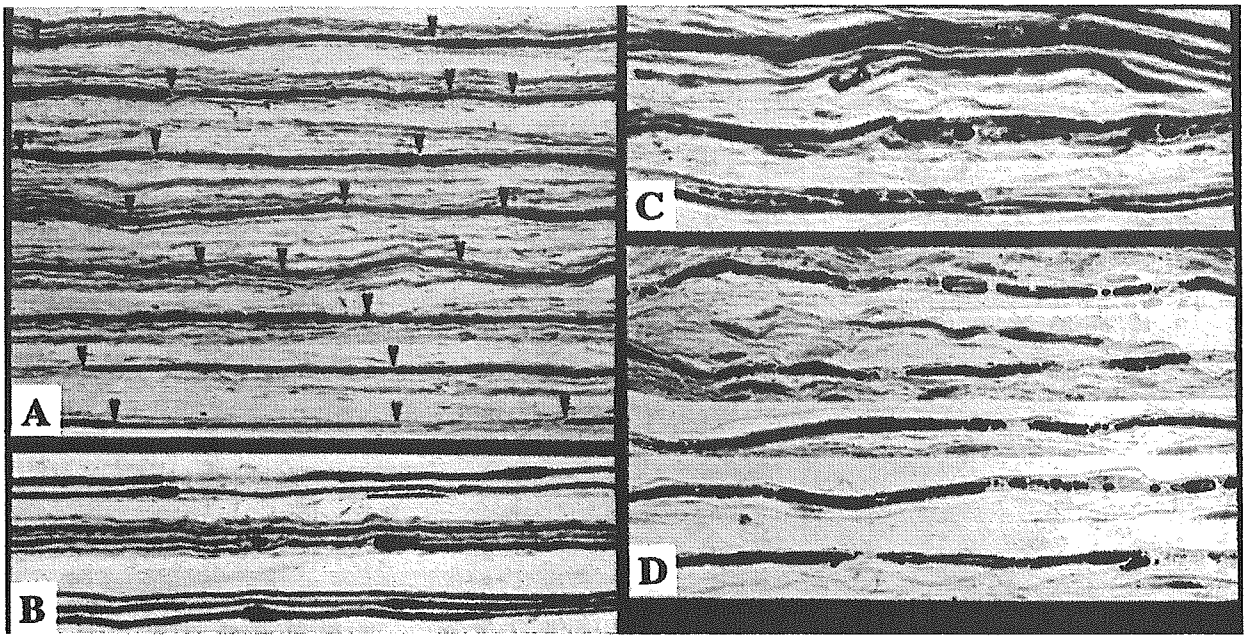

Fig. 4 (A) Teased fibres from the sural nerves of CMT patients. Extensive segmental demyelination was observed in a fibre from a patient with PMP22 duplication. Arrowheads indicate the node of Ranvier. (B) Globule or tomacula formation was abundant in another patient with PMP22 duplication. (C and D) Fibres with axonal degeneration were seen in an axonal subgroup of patients with an MPZ mutation (Thy124Met) (C) and in a patient with a Cx32 mutation (Phe69Leu) (D). Magnification: A, ×100; B, ×80; C and D, ×150.

In contrast, MCVs of median, ulnar and tibial nerves did not correlate with distal muscle strength in patients with PMP22 duplication, MPZ mutations or Cx32 mutations. These findings indicate that weakness in distal limb muscles was a consequence of reduced CMAP amplitude, not the slowing of MCV, in all groups.

Discussion

In CMT patients with PMP22 duplication, almost all patients showed predominantly demyelinating features in the nerve conduction study and pathological examination, with variable severity among individuals. MCVs were ≤38 m/s, independently of age and disease duration. However, features of axonal loss, axonal sprouts and axonal changes in teased-fibre preparations as well as the decrease in CMAP amplitude were variably present irrespective of marked slowing of nerve conduction. These observations were in good agreement with previous reports (Kaku *et al.*, 1993*a*; Thomas *et al.*, 1997; Birouk *et al.*, 1997; Garcia *et al.*, 1998; Krajewski *et al.*, 2000; Dubourg *et al.*, 2001*a*). Since PMP22 duplication was shared among these patients, variability of demyelinating and axonal pathology between individual patients must be attributed to factors other than PMP22 duplication. Important factors demonstrated in this study were age and disease duration. CMAP reduction, axonal loss and onion bulb formation were more pronounced in advanced disease. Other factors could be the genetic background or environmental differences, as demonstrated in previous reports showing that the degree of reduction of nerve conduction was variable even in a family pedigree and in identical twins (Kaku *et al.*, 1993*a*, *b*; Garcia *et al.*, 1995, 1998; Birouk *et al.*, 1997). As reported so far, PMP22 duplication thus induces a mainly demyelinating phenotype, while features of axonal pathology are present concomitantly with advancing disease.

In cases with MPZ mutations, axonal and demyelinating phenotypes were clearly differentiated into two subgroups. Patients in the axonal subgroup rarely showed concomitant demyelinating phenotypes, and patients in the demyelinating subgroup rarely showed axonal features. These axonal or demyelinating phenotypes were also concordant among siblings in individual families. Furthermore, the nature and position of the MPZ gene mutation did not overlap between these two subgroups, indicating that axonal or demyelinating phenotypes are determined mainly by the nature and position of mutations of the MPZ gene. Apart from the MPZ gene mutation, the overall genetic background and environmental factors may have little effect on phenotypic variation in patients with the MPZ mutation. Age- and duration-dependent clinical and pathological changes could also be present, as was seen for PMP22 duplication, but we could not assess these issues because of relatively small numbers of patients in the subgroups.

Frequent association of neural deafness and pupillary abnormality in patients with the axonal phenotype of MPZ mutations was characteristic, confirming previous observations (Chapon *et al.*, 1999; De Jonghe *et al.*, 1999; Misu *et al.*, 2000). Prominent serum CK elevation was also more frequent

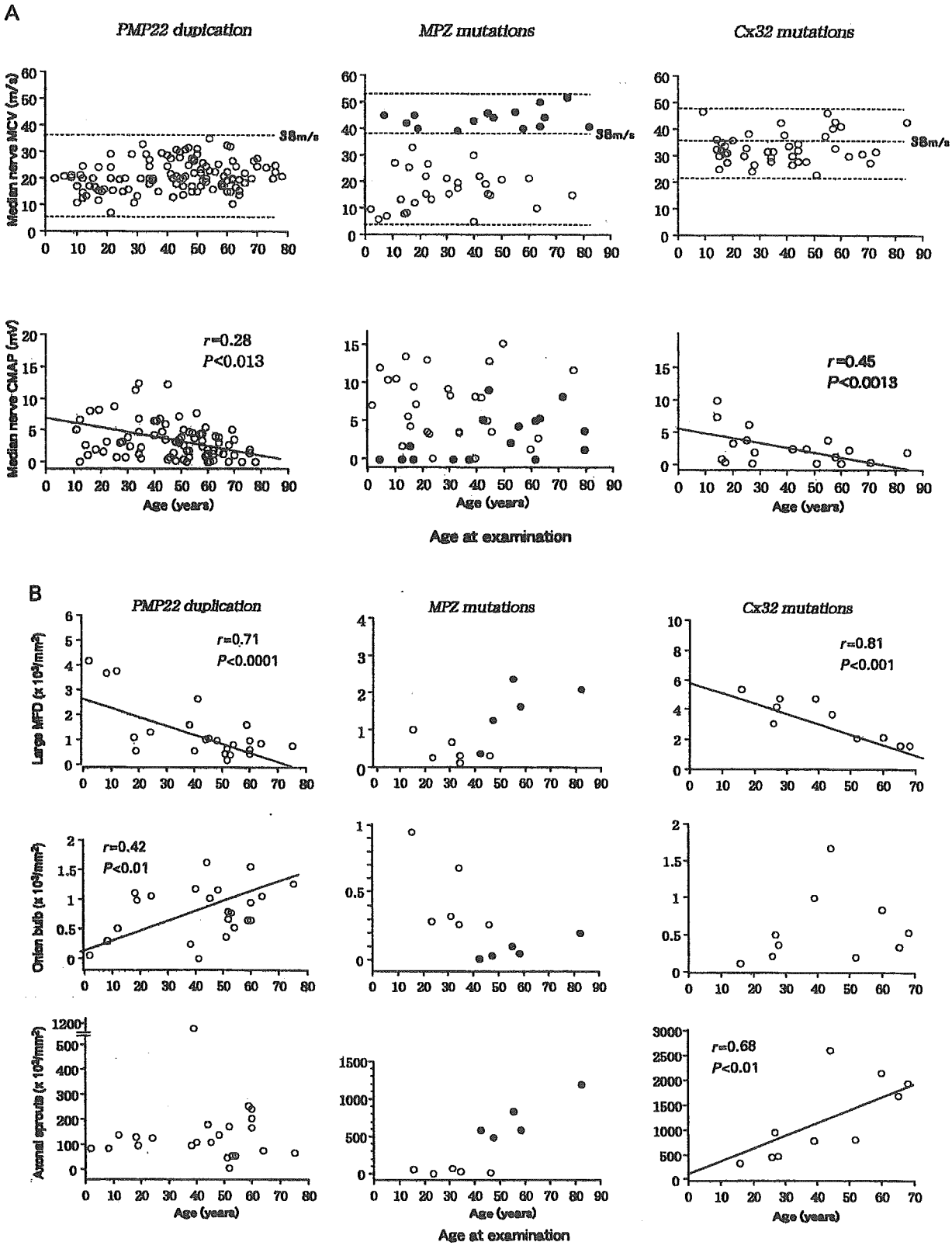

Fig. 5 Scattergrams of median nerve MCVs, CMAPs (A) and sural nerve pathology (B) in relation to age at examination in CMT patients. Closed circles and open circles in the panel labelled 'MPZ mutations' indicate patients with median nerve MCVs >38 m/s (corresponding to axonal phenotypes) and ≤38 m/s (corresponding to demyelinating phenotypes), respectively. In A, the dotted lines indicate the maximum and minimum values in each scattergram, and the 38 m/s level.

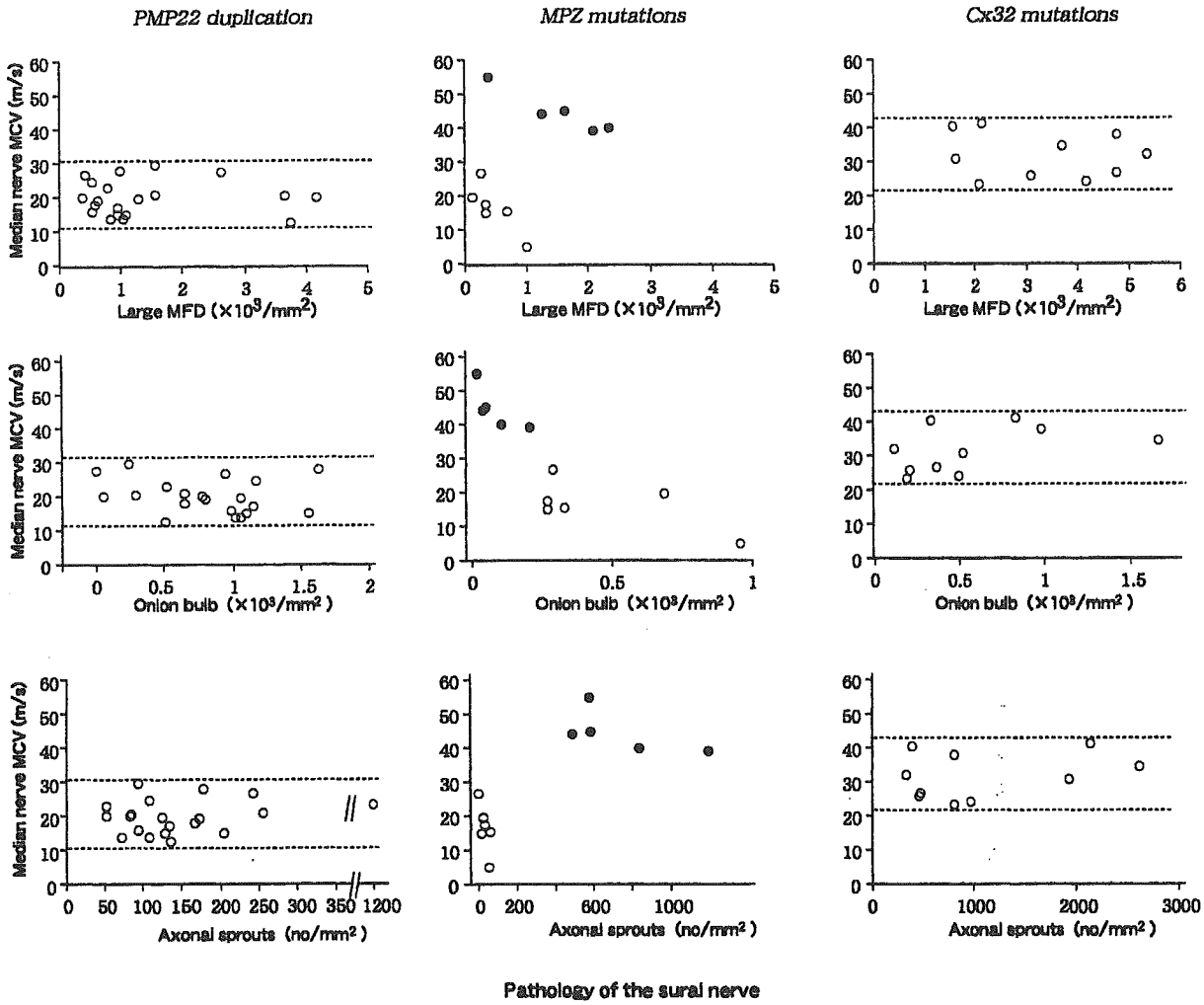

Fig. 6 Scattergrams of median nerve MCVs in relation to severity of sural nerve pathology [large myelinated fibre density (MFD), density of onion bulbs and axonal sprouts]. Closed circles and open circles in the panel labelled 'MPZ mutations' indicate patients with median nerve MCVs >38 m/s (corresponding to axonal phenotypes) and ≤38 m/s (corresponding to demyelinating phenotypes), respectively. Dotted lines indicate the maximum and minimum values in each scattergram.

in patients with MPZ mutation in the axonal subgroup. These associated symptoms were not restricted to specific MPZ mutations, but were widely present among patients with axonal phenotypes. These observations suggest that the mechanism that induces the axonal phenotype may also induce associated symptoms.

In Cx32 mutations, median nerve MCV was moderately slowed within a relatively restricted range of 22.8–46.6 m/s, confirming previous reports (Hahn *et al.*, 1990; Nicholson *et al.*, 1993, 1998; Dubourg *et al.*, 2001*a*, *b*). Pathologically, axonal features predominated but demyelinating features were present concomitantly, suggesting a mixture of axonal and demyelinating pathology. These MCVs and pathological phenotypes were independent of age and disease duration. However, other axonal markers, such as decreased CMAP amplitudes, axonal loss and axonal sprouts, were pronounced in patients with advanced disease. Cx32 mutations may induce both axonal and demyelinating features irrespective of the nature and position of the mutation in the Cx32 gene, with median MCVs showing a moderately decreased range.

Strikingly, median nerve MCVs were consistent independently of age, disease duration and pathological alterations in all three groups of genetic abnormality (Table 6). By consensus, the division point for axonal and demyelinating phenotypes of CMT has been considered to be 38 m/s for median nerve MCV (Dyck and Lambert, 1968; Buchthal and Behse, 1977; Harding and Thomas, 1980). Nerve conduction criteria for axonal and demyelinating phenotypes have been verified by observations in PMP22 duplication (Kaku *et al.*, 1993*a*, *b*; Nicholson and Nash, 1993; Nicholson *et al.*, 1998; Paraskevas *et al.*, 1998). In this study we confirmed the usefulness of this nerve conduction cut-off value in MPZ mutations. However, in Cx32 mutations, 38 m/s for median nerve MCV was not a useful division point. Median nerve

Table 4 *Gene mutations and median nerve MCV and concordance and discordance among siblings*

Gene mutations and median nerve MCV in the proband	Mutations	No. of families; MCV concordance and discordance among siblings in families examined systemically		
		Concordance to MCV ≤38 m/s	Concordance to MCV >38 m/s	Discordance to MCV ≤38 m/s and MCV >38 m/s
PMP22 duplication	Duplication of PMP22 gene	18 (2–5)	0	0
MPZ mutations				
MCV ≤38 m/s	Asp35Tyr, Ile62Phe, Ser63del, Tyr68Cys, Gly93Glu, Arg98Cys, Val146Phe	4 (2–4)	0	0
MCV >38 m/s	Asp75Val, His81Arg, Thr124Met Lys130Arg, Gly167Arg	0	4 (2–3)	0
Cx32 mutations	Ser26Leu, Thr55Ala, Gln57His, Val63Ile, Phe69Leu, Ser128stop, Val139Met, Arg142Gln, Arg142Trp, Pro172Arg, Val177Ala, Arg183His, Thr191Ala, Cys201Tyr, Ala282frameshift	1 (2)	0	6 (2–3)

Numbers in parentheses are number of patients in the family whose median nerve MCV was estimated.

Table 5 *Correlation between CMAP/MCV and muscle strength*

Mutations/nerves	*n*	*r*	*P*
PMP22 duplication			
Median			
CMAP vs distal MS	86	0.35	<0.0009
MCV vs distal MS	86	0.16	NS
Ulnar			
CMAP vs distal MS	63	0.44	<0.0005
MCV vs distal MS	63	0.05	NS
Posterior tibialis			
CMAP vs distal MS	79	0.36	<0.0014
MCV vs distal MS	79	0.15	NS
MPZ mutations			
Median			
CMAP vs distal MS	28	0.36	<0.05
MCV vs distal MS	28	0.05	NS
Ulnar			
CMAP vs distal MS	17	0.43	<0.05
MCV vs distal MS	17	0.14	NS
Posterior tibialis			
CMAP vs distal MS	17	0.47	<0.018
MCV vs distal MS	17	0.17	NS
Cx32 mutations			
Median			
CMAP vs distal MS	19	0.69	<0.0032
MCV vs distal MS	19	0.21	NS
Ulnar			
CMAP vs distal MS	19	0.68	<0.0079
MCV vs distal MS	19	0.30	NS
Posterior tibial			
CMAP vs distal MS	19	0.38	NS
MCV vs distal MS	19	0.16	NS

MS = muscle strength assessed as MRC score; distal MS = thenar and finger flexion muscles for the median nerves, interosseous muscles for the ulnar nerves, and triceps surae muscles and toe dorsiflexion muscles for the posterior tibial nerve. MS was assessed as MRC score for the examined muscles and averaged for the examined muscles for each individual.

MCV for Cx32 mutations ranged around 38 m/s but was restricted to a range between 22.8 and 46.6 m/s. The observation that median nerve MCVs are well maintained independently of age, disease duration and clinicopathological changes indicates that median nerve MCV is an excellent marker for genetically determined CMT phenotypes. In contrast, the amplitude of CMAPs, axonal loss (particularly for large axons), the density of axonal sprouts and onion bulb formation changed significantly with age and disease duration (Table 6). Distally accentuated muscular wasting was characteristic of all three genotypes and progressed with advancing age (Dyck *et al.*, 1989; Birouk *et al.*, 1997), showing good correlation with CMAP amplitude in the corresponding muscles. Disease duration, however, correlated less well with these features than did age at examination, suggesting that the disease process may begin early, at perinatal or embryonic stages, as suggested previously (Dyck *et al.*, 1989; Killian *et al.*, 1996; Garcia *et al.*, 1998). Disease duration, which represents the period after the disease process has crossed the clinical threshold, appears to correlate less well with the pathological changes and CMAPs than age at examination. Age-dependent decreases in CMAPs and increases in axonal pathology and clinical disability from neuropathic deficits were in good agreement with previous observations in CMT1 patients (Dyck *et al.*, 1989).

Taking all the results in this study together, we can identify two distinct clinicopathological phenotypic features, one that is independent of disease advancement and the other with changing phenotypic features according to disease advancement. The MCVs and the predominance of demyelinating or axonal phenotypes are included in the former category, and axonal features, such as CMAP amplitude, large-axon loss, axonal sprouts and distally accentuated muscle wasting, are included in the latter category. The present study shows that axonal features that change in relation to disease advance-

Table 6 *Demyelinating and axonal features of CMT patients*

Mutations	Disease advancement		Disease advancement-dependent				Correlation to muscle wasting
	Median nerve MCV	Predominant pathological phenotype	Decrease in CMAP	Axon loss	Axonal sprouts	Onion bulbs	
PMP22 duplication	≤38 m/s	Demyelinating	Yes	Yes	No	Yes	CMAP
MPZ mutations	≤38 m/s	Demyelinating	ND	ND	ND	ND	CMAP
	>38 m/s	Axonal	ND	ND	ND	ND	CMAP
Cx32 mutations	22.8 to 46.6 m/s	Axonal with mild demyelinating	Yes	Yes	Yes	No	CMAP

ND, not determined (sample size too small).

ment, particularly large-axon loss and decreased CMAP amplitude, constitute a major determinant of clinical manifestations such as muscle weakness and atrophy in all three common genotypic groups of CMT.

The molecular mechanisms that induce axonal involvement as disease advances, which have been demonstrated particularly in PMP22 duplication and Cx32 mutations, are poorly understood, and may differ among mutations. In the case of PMP22 duplication, axonal dysfunction could result from the primary process of demyelination, as suggested in previous studies (Dyck *et al.*, 1989; Garcia *et al.*, 1998; Sancho *et al.*, 1999; Scherer, 1999; Krajewski *et al.*, 2000). Local biochemical changes in axons, such as decreased neurofilament phosphorylation, increased neurofilament density and decreased axonal transport due to demyelinating Schwann cells, could accrue to produce axonal dysfunction and eventual axonal loss (de Waegh and Brady, 1990, de Waegh *et al.*, 1992; Watson *et al.*, 1994; Sahenk *et al.*, 1999). In Cx32 mutations, issues concerning mechanisms of progressive axonal involvement are further complicated, since an axonal phenotype is predominant but demyelinating features are concomitantly present to variable degrees in individual patients. Unknown mechanisms may induce axonal dysfunction and loss directly, while concomitant demyelinating features could also induce axon loss, as is suspected for PMP22 duplication. Studies using *in vivo* models with specific mutations of Cx32 and different genetic or environmental backgrounds are needed to provide better understanding of the molecular mechanisms.

The distally accentuated muscle wasting characteristic of CMT was strongly correlated with the reduction of the functioning large axonal population, as assessed by CMAPs, and was not correlated with slowing of nerve conduction. This finding was common to patients with PMP22 duplication, MPZ mutations and Cx32 mutations. Similar observations were reported in patients with PMP22 duplication (Krajewski *et al.*, 2000). In that report, muscle wasting and sensory impairment that was accentuated in the distal extremities correlated well with corresponding reductions in CMAPs and SNAPs, but not with slowing of motor and sensory nerve conduction. Our observations are in agreement with these reported observations in PMP22 duplication, while we have demonstrated further that clinical phenotypes of patients with MPZ and Cx32 mutations are also determined by reduction of the functioning large-axon population. Pathological study of autopsy cases of CMT with a hypertrophic form of extensive demyelination and an axonal form with massive axonal sprouting both demonstrated distally accentuated axon loss along peripheral nerve trunks that showed relatively well-preserved axons proximally (Smith *et al.*, 1980; Berciano *et al.*, 1986; Bird *et al.*, 1997). These pathological observations in CMT patients showing distally pronounced axon loss irrespective of the axonal or demyelinating phenotypes agree with the present study in showing distally accentuated muscle wasting in both axonal and demyelinating phenotypes.

In conclusion, our study demonstrates that three myelin-related protein gene abnormalities, PMP22 duplication, MPZ mutations and Cx32 mutations, resulted in a wide variety of demyelinating and axonal features. PMP22 duplication induced demyelinating changes; MPZ mutations induced distinctive subgroups with a demyelinating or axonal phenotype depending on the nature and position of the mutation; and Cx32 mutations induced predominant axonal and lesser demyelinating features essentially simultaneously. These genetically determined axonal and demyelinating phenotypes corresponded well with median nerve MCVs, which remained constant despite disease advancement. In contrast, clinical manifestations of muscle wasting correlated well with decreases in CMAPs and axonal loss, which became more pronounced as disease progressed.

Acknowledgements

This work was supported by a COE grant from the Ministry of Education, Science, Culture and Sports of Japan and grants from the Ministry of Health, Labour and Welfare of Japan. The following members of the Study Group for Hereditary Neuropathy in Japan were supported by the Ministry of

Health, Labour, and Welfare of Japan: Gen Sobue, Department of Neurology, Nagoya University Graduate School of Medicine; Ichiro Akiguchi, Department of Neurology, Kyoto University Graduate School of Medicine; Kiyoshi Hayasaka, Department of Pediatrics, Yamagata University School of Medicine; Masanori Nakagawa, Third Department of Internal Medicine, Kagoshima University Faculty of Medicine; Saburo Sakota, Department of Neurology, Osaka University Graduate School of Medicine; Kiichiro Matsumura, Department of Neurology, Teikyo University School of Medicine; Satoshi Onodera, Department of Neurology, Niigata University Graduate School of Medicine and Dental Sciences; Shu-ichi Ikeda, Department of Internal Medicine, Shinshu University School of Medicine; Takashi Yamamura, Department of Immunology, National Center of Neurology and Psychiatry; Yukio Ando, Department of Neurology, Kumamoto University School of Laboratory Medicine; Masayuki Baba, Department of Neurology, Hirosaki University School of Medicine; Masamitsu Nakazato, Third Department of Internal Medicine, Miyazaki Medical College; Hitoshi Yasuda, Third Department of Internal Medicine, Shiga University of Medical Sciences; Toyokazu Saito, Department of Neurology, Kitasato University School of Medicine; Kazuhiro Ikenaka, Department of Neural Information, National Institute for Physiology Laboratory; Jun-ichi Kira, Department of Neurology, Kyushu University Graduate School of Medicine; Keiji Wada, Department of Degenerative Neurological Diseases, National Center for Neurology and Psychiatry; Kenji Nakashima, Department of Neurological Sciences, Tottori University Faculty of Medicine; Kazuhiko Watabe, Department of Molecular Neuropathology, Tokyo Metropolitan Institute for Neurosciences; Ryuji Kaji, Division of Advanced Clinical Neuroscience, University of Tokushima School of Medicine; Nobuyuki Oka, Department of Internal Medicine, Hyogo College of Medicine; Eiko Ando, Department of Ophthalmology, Kumamoto National Hospital.

References

Baxter RV, Ben Othmane K, Rochelle JM, Stajich JE, Hulette C, Dew-Knight S, et al. Ganglioside-induced differentiation-associated protein-1 is mutant in Charcot–Marie–Tooth disease type 4A/8q21. Nature Genet 2002; 30: 21–2.

Berciano J, Combarros O, Figols J, Calleja J, Cabello A, Silos I, et al. Hereditary motor and sensory neuropathy type II. Clinicopathological study of a family. Brain 1986; 109: 897–914.

Bergoffen J, Scherer SS, Wang S, Scott MO, Bone LJ, Paul DL, et al. Connexin mutation in X-linked Charcot–Marie–Tooth disease. Science 1993; 262: 2039–42.

Bird TD, Kraft GH, Lipe HP, Kenney KL, Sumi SM. Clinical and pathological phenotype of the original family with Charcot–Marie–Tooth type 1B: a 20-year study. Ann Neurol 1997; 41: 463–9.

Birouk N, Gouider R, LeGuern E, Gugenheim M, Tardieu S, Maisonobe T, et al. Charcot–Marie–Tooth disease type 1A with 17p11.2 duplication. Clinical and electrophysiological phenotype study and factors influencing disease severity in 119 cases. Brain 1997; 120: 813–23.

Birouk N, LeGuern E, Maisonobe T, Rouger H, Gouider R, Tardieu S, et al. X-linked Charcot–Marie–Tooth disease with connexin32 mutations. Clinical and electrophysiologic study. Neurology 1998; 50: 1074–82.

Boerkoel CF, Takashima H, Garcia CA, Olney RK, Johnson J, Berry K, et al. Charcot–Marie–Tooth disease and related neuropathies: mutation distribution and genotype–phenotype correlation. Ann Neurol 2002; 51: 190–201.

Bolino A, Muglia M, Conforti FL, LeGuern E, Salih MA, Georgiou DM, et al. Charcot–Marie–Tooth type 4B is caused by mutations in the gene encoding myotubularin-related protein-2. Nature Genet 2000; 25: 17–9.

Bradley WG, Madrid R, Davis CJ. The peroneal muscular atrophy syndrome. J Neurol Sci 1977; 32: 123–36.

Buchthal F, Behse F. Peroneal muscular atrophy (PMA) and related disorders. I. Clinical manifestations as related to biopsy findings, nerve conduction and electromyography. Brain 1977; 100: 41–66.

Chapon F, Latour P, Diraison P, Schaeffer S, Vandenberghe A. Axonal phenotype of Charcot–Marie–Tooth disease associated with a mutation in the myelin protein zero gene. J Neurol Neurosurg Psychiatry 1999; 66: 779–82.

Cuesta A, Pedrola L, Sevilla T, Garcia-Planells J, Chumillas MJ, Mayordomo F, et al. The gene encoding ganglioside-induced differentiation-associated protein1 is mutated in axonal Charcot–Marie–Tooth type 4A disease. Nature Genet 2002; 30: 22–5.

De Jonghe P, Timmerman V, Ceuterick C, Nelis E, De Vriendt E, Lofgren A, et al. The Thr124Met mutation in the peripheral myelin protein zero (MPZ) gene is associated with a clinically distinct Charcot–Marie–Tooth phenotype. Brain 1999; 122: 281–90.

De Sandre-Giovannoli A, Chaouch M, Kozlov S, Vallat JM, Tazir M, Kassouri N, et al. Homozygous defects in LMNA, encoding lamin A/C nuclear-envelope proteins, cause autosomal recessive axonal neuropathy in human (Charcot–Marie–Tooth disease type 2) and mouse. Am J Hum Genet 2002; 70: 726–36.

de Waegh S, Brady ST. Altered slow axonal transport and regeneration in myelin-deficient mutant mouse: the trembler as an in vivo model for Schwann cell-axon interactions. J Neurosci 1990; 10: 1855–65.

de Waegh SM, Lee VM, Brady ST. Local modulation of neurofilament phosphorylation, axonal caliber, and slow axonal transport by myelinating Schwann cells. Cell 1992; 68: 451–63.

Dubourg O, Tardieu S, Birouk N, Gouider R, Leger JM, Maisonobe T, et al. Clinical, electrophysiological and molecular genetic characteristics of 93 patients with X-linked Charcot–Marie–Tooth disease. Brain 2001a; 124: 1958–67.

Dubourg O, Tardieu S, Birouk N, Gouider R, Leger JM, Maisonobe T, et al. The frequency of 17p11.2 duplication and Connexin 32 mutations in 282 Charcot–Marie–Tooth families in relation to the mode of inheritance and motor nerve conduction velocity. Neuromuscul Disord 2001b; 11: 458–63.

Dyck PJ, Lambert EH. Lower motor and primary sensory neuron diseases with peroneal muscular atrophy. I. Neurologic, genetic, and electrophysiologic findings in hereditary polyneuropathies. Arch Neurol 1968; 18: 603–18.

Dyck PJ, Karnes JL, Lambert EH. Longitudinal study of neuropathic deficits and nerve conduction abnormalities in hereditary motor and sensory neuropathy type 1. Neurology 1989; 39: 1302–8.

Dyck PJ, Giannini C, Lais A. Pathologic alterations of nerves. In: Dyck PJ, Thomas PK, Griffin JW, Low PA, Poduslo JF, editors. Peripheral neuropathy. 3rd ed. Philadelphia: W.B. Saunders; 1993. p. 514–95.

Gabreels-Festen AA, Hoogendijk JE, Meijerink PH, Gabreels FJ, Bolhuis PA, van Beersum S, et al. Two divergent types of nerve pathology in patients with different P0 mutations in Charcot–Marie–Tooth disease. Neurology 1996; 47: 761–5.

Garcia CA, Malamut RE, England JD, Parry GS, Liu P, Lupski JR. Clinical variability in two pairs of identical twins with the Charcot–Marie–Tooth disease type 1A duplication. Neurology 1995; 45: 2090–3.

Garcia A, Combarros O, Calleja J, Berciano J. Charcot–Marie–Tooth disease type 1A with 17p duplication in infancy and early childhood: a longitudinal clinical and electrophysiologic study. Neurology 1998; 50: 1061–7.

Guilbot A, Williams A, Ravise N, Verny C, Brice A, Sherman DL, et al. A mutation in periaxin is responsible for CMT4F, an autosomal recessive form of Charcot–Marie–Tooth disease. Hum Mol Genet 2001; 10: 415–21.

Gutierrez A, England JD, Sumner AJ, Ferer S, Warner LE, Lupski JR, et al. Unusual electrophysiological findings in X-linked dominant Charcot–Marie–Tooth disease. Muscle Nerve 2000; 23: 182–8.

Hahn AF, Brown WF, Koopman WJ, Feasby TE. X-linked dominant hereditary motor and sensory neuropathy. Brain 1990; 113: 1511–25.

Hahn AF, Ainsworth PJ, Bolton CF, Bilbao JM, Vallat JM. Pathological findings in the x-linked form of Charcot–Marie–Tooth disease: a morphometric and ultrastructural analysis. Acta Neuropathol (Berl) 2001; 101: 129–39.

Harding AE. From the syndrome of Charcot, Marie and Tooth to disorders of peripheral myelin proteins. [Review]. Brain 1995; 118: 809–18.

Harding AE, Thomas PK. The clinical features of hereditary motor and sensory neuropathy types I and II. Brain 1980; 103: 259–80.

Hattori N, Ichimura M, Nagamatsu M, Li M, Yamamoto K, Kumazawa K, et al. Clinicopathological features of Churg–Strauss syndrome-associated neuropathy. Brain 1999; 122: 427–39.

Hayasaka K, Himoro M, Sato W, Takada G, Uyemura K, Shimizu N, et al. Charcot–Marie–Tooth neuropathy type 1B is associated with mutation of the myelin P0 gene. Nature Genet 1993; 5: 31–4.

Ikegami T, Ikeda H, Chance PF, Kiyosawa H, Yamamoto M, Sobue G, et al. Facilitated diagnosis of the CMT1A duplication in chromosome 17p11.2–12: analysis with a CMT1A-REP repeat probe and photostimulated luminescence imaging. Hum Mutat 1997; 9: 563–6.

Ionasescu V, Searby C, Ionasescu R. Point mutations of the connexin32 (GJB1) gene in X-linked dominant Charcot–Marie–Tooth neuropathy. Hum Mol Genet 1994; 3: 355–8.

Ionasescu VV, Searby C, Ionasescu R, Neuhaus IM, Werner R. Mutations of the noncoding region of the connexin32 gene in X-linked dominant Charcot–Marie–Tooth neuropathy. Neurology 1996; 47: 541–4.

Kaku DA, Parry GJ, Malamut R, Lupski JR, Garcia CA. Nerve conduction studies in Charcot–Marie–Tooth polyneuropathy associated with a segmental duplication of chromosome 17. Neurology 1993a; 43: 1806–8.

Kaku DA, Parry GJ, Malamut R, Lupski JR, Garcia CA. Uniform slowing of conduction velocities in Charcot–Marie–Tooth polyneuropathy type 1. Neurology 1993b; 43: 2664–7.

Kalaydjieva L, Gresham D, Gooding R, Heather L, Baas F, de Jonge R, et al. N-myc downstream-regulated gene 1 is mutated in hereditary motor and sensory neuropathy-Lom. Am J Hum Genet 2000; 67: 47–58.

Kamholz J, Menichella D, Jani A, Garbern J, Lewis RA, Krajewski KM, et al. Charcot–Marie–Tooth disease type 1: molecular pathogenesis to gene therapy. [Review]. Brain 2000; 123: 222–33.

Killian JM, Tiwari PS, Jacobson S, Jackson RD, Lupski JR. Longitudinal studies of the duplication form of Charcot–Marie–Tooth polyneuropathy. Muscle Nerve 1996; 19: 74–8.

Koike H, Mori K, Misu K, Hattori N, Ito H, Hirayama M, et al. Painful alcoholic polyneuropathy with predominant small-fiber loss and normal thiamine status. Neurology 2001; 56: 1727–32.

Kovach MJ, Lin JP, Boyadjiev S, Campbell K, Mazzeo L, Herman K, et al. A unique point mutation in the PMP22 gene is associated with Charcot–Marie–Tooth disease and deafness. Am J Hum Genet 1999; 64: 1580–93.

Krajewski KM, Lewis RA, Fuerst DR, Turansky C, Hinderer SR, Garbern J, et al. Neurological dysfunction and axonal degeneration in Charcot–Marie–Tooth disease type 1A. Brain 2000; 123: 1516–27.

Lupski JR, de Oca-Luna RM, Slaugenhaupt S, Pentao L, Guzzetta V, Trask BJ, et al. DNA duplication associated with Charcot–Marie–Tooth disease type 1A. Cell 1991; 66: 219–32.

Marrosu MG, Vaccargiu S, Marrosu G, Vannelli A, Cianchetti C, Muntoni F. Charcot–Marie–Tooth disease type 2 associated with mutation of the myelin protein zero gene. Neurology 1998; 50: 1397–401.

Matsunami N, Smith B, Ballard L, Lensch MW, Robertson M, Albertsen H, et al. Peripheral myelin protein-22 gene maps in the duplication in chromosome 17p11.2 associated with Charcot–Marie–Tooth 1A. Nature Genet 1992; 1: 176–9.

Mersiyanova IV, Perepelov AV, Polyakov AV, Sitnikov VF, Dadali EL, Oparin RB, et al. A new variant of Charcot–Marie–Tooth disease type 2 is probably the result of a mutation in the neurofilament-light gene. Am J Hum Genet 2000; 67: 37–46.

Misu K, Hattori N, Nagamatsu M, Ikeda S, Ando Y, Nakazato M, et al. Late-onset familial amyloid polyneuropathy type I (transthyretin Met30-associated familial amyloid polyneuropathy)

unrelated to endemic focus in Japan: clinicopathological and genetic features. Brain 1999; 122: 1951–62.

Misu K, Yoshihara T, Shikama Y, Awaki E, Yamamoto M, Hattori N, et al. An axonal form of Charcot–Marie–Tooth disease showing distinctive features in association with mutations in the peripheral myelin protein zero gene (Thr124Met or Asp75Val). J Neurol Neurosurg Psychiatry 2000; 69: 806–11.

Nagarajan R, Svaren J, Le N, Araki T, Watson M, Milbrandt J. EGR2 mutations in inherited neuropathies dominant-negatively inhibit myelin gene expression. Neuron 2001; 30: 355–68.

Nelis E, Van Broeckhoven C, De Jonghe P, Lofgren A, Vandenberghe A, Latour P, et al. Estimation of the mutation frequencies in Charcot–Marie–Tooth disease type 1 and hereditary neuropathy with liability to pressure palsies: a European collaborative study. Eur J Hum Genet 1996; 4: 25–33.

Nicholson G, Nash J. Intermediate nerve conduction velocities define X-linked Charcot–Marie–Tooth neuropathy families. Neurology 1993; 43: 2558–64.

Nicholson GA, Yeung L, Corbett A. Efficient neurophysiologic selection of X-linked Charcot–Marie–Tooth families: ten novel mutations. Neurology 1998; 51: 1412–6.

Paraskevas GP, Panousopoulou A, Karandreas N, Piperos P, Lygidakis C, Papageorgiou C. Correlation between denervation activity and compound muscle action potential amplitude in hereditary motor and sensory neuropathy I and II. Electromyogr Clin Neurophysiol 1998; 38: 343–7.

Patel PI, Roa BB, Welcher AA, Schoener-Scott R, Trask BJ, Pentao L, et al. The gene for the peripheral myelin protein PMP-22 is a candidate for Charcot–Marie–Tooth disease type 1A. Nature Genet 1992; 1: 159–65.

Raeymaekers P, Timmerman V, Nelis E, De Jonghe P, Hoogendijk JE, Baas F, et al. Duplication in chromosome 17p11.2 in Charcot–Marie–Tooth neuropathy type 1a (CMT 1a). The HMSN Collaborative Research Group. Neuromuscul Disord 1991; 1: 93–7.

Reilly MM. Classification of the hereditary motor and sensory neuropathies. [Review]. Curr Opin Neurol 2000; 13: 561–4.

Sahenk Z, Chen L, Mendell JR. Effects of PMP22 duplication and deletions on the axonal cytoskeleton. Ann Neurol 1999; 45: 16–24.

Sancho S, Magyar JP, Aguzzi A, Suterl U. Distal axonopathy in peripheral nerves of PMP22-mutant mice. Brain 1999; 122: 1563–77.

Sander S, Nicholson GA, Ouvrier RA, McLeod JG, Pollard JD. Charcot–Marie–Tooth disease: histopathological features of the peripheral myelin protein (PMP22) duplication (CMT1A) and connexin32 mutations (CMTX1). Muscle Nerve 1998; 21: 217–25.

Sander S, Ouvrier RA, Mcleod JG, Nicholson GA, Pollard JD. Clinical syndromes associated with tomacula or myelin swellings in sural nerve biopsies. J Neurol Neurosurg Psychiatry 2000; 68: 483–8.

Scherer S. Axonal pathology in demyelinating diseases [letter]. Ann Neurol 1999; 45: 6–7.

Scherer SS, Fischbeck KH. Is CMTX an axonopathy? [letter]. Neurology 1999; 52: 432–3.

Senderek J, Hermanns B, Bergmann C, Boroojerdi B, Bajbouj M, Hungs M, et al. X-linked dominant Charcot–Marie–Tooth neuropathy: clinical, electrophysiological, and morphological phenotype in four families with different connexin32 mutations (1). J Neurol Sci 1999; 167: 90–101.

Smith TW, Bhawan J, Keller RB, DeGirolami U. Charcot–Marie–Tooth disease associated with hypertrophic neuropathy: a neuropathologic study of two cases. J Neuropathol Exp Neurol 1980; 39: 420–40.

Sobue G, Hashizume Y, Mukai E, Hirayama M, Mitsuma T, Takahashi A, et al. X-Linked recessive bulbospinal neuronopathy: a clinicopathological study. Brain 1989; 112: 209–32.

Sobue G, Nakao N, Murakami K, Yasuda T, Sahashi K, Mitsuma T, et al. Type I familial amyloid polyneuropathy. A pathological study of the peripheral nervous system. Brain 1990; 113: 903–19.

Sobue G, Li M, Terao S, Aoki S, Ichimura M, Ieda T, et al. Axonal pathology in Japanese Guillain-Barré syndrome: a study of 15 autopsied cases. Neurology 1997; 48: 1694–700.

Tabaraud F, Lagrange E, Sindou P, Vandenberghe A, Levy N, Vallat JM. Demyelinating X-linked Charcot–Marie–Tooth disease: unusual electrophysiological findings. Muscle Nerve 1999; 22: 1442–7.

Thomas PK, Marques W Jr, Davis MB, Sweeney MG, King RH, Bradley JL, et al. The phenotypic manifestations of chromosome 17p11.2 duplication. Brain 1997; 120: 465–78.

Timmerman V, Nelis E, Van Hul W, Nieuwenhuijsen BW, Chen KL, Wang S, et al. The peripheral myelin protein gene PMP-22 is contained within the Charcot–Marie–Tooth disease type 1A duplication. Nature Genet 1992; 1: 171–5.

Vital A, Ferrer X, Lagueny A, Vandenberghe A, Latour P, Goizet C, et al. Histopathological features of X-linked Charcot–Marie–Tooth disease in 8 patients from 6 families with different connexin32 mutations. J Peripher Nerv Syst 2001; 6: 79–84.

Warner LE, Mancias P, Butler IJ, McDonald CM, Keppen L, Koob KG, et al. Mutations in the early growth response 2 (EGR2) gene are associated with hereditary myelinopathies. Nature Genet 1998; 18: 382–4.

Watson DF, Nachtman FN, Kuncl RW, Griffin JW. Altered neurofilament phosphorylation and beta tubulin isotypes in Charcot–Marie–Tooth disease type I. Neurology 1994; 44: 2383–7.

Yamamoto M, Yasuda T, Hayasaka K, Ohnishi A, Yoshikawa H, Yanagihara T, et al. Locations of crossover breakpoints within the CMT1A-REP repeat in Japanese patients with CMT1A and HNPP. Hum Genet 1997; 99: 151–4.

Yamamoto M, Keller MP, Yasuda T, Hayasaka K, Ohnishi A, Yoshikawa H, et al. Clustering of CMT1A duplication breakpoints in a 700 bp interval of the CMT1A-REP repeat. Hum Mutat 1998; 11: 109–13.

Yoshihara T, Yamamoto M, Doyu M, Mis KI, Hattori N, Hasegawa Y, et al. Mutations in the peripheral myelin protein zero and connexin32 genes detected by non-isotopic RNase cleavage assay and their phenotypes in Japanese patients with Charcot–Marie–Tooth disease. Hum Mutat (Online) 2000; 16: 177–8.

Yoshihara T, Kanda F, Yamamoto M, Ishihara H, Misu K, Hattori N, et al. A novel missense mutation in the early growth response 2 gene associated with late-onset Charcot–Marie–Tooth disease type 1. J Neurol Sci 2001; 184: 149–53.

Zhao C, Takita J, Tanaka Y, Setou M, Nakagawa T, Takeda S, et al. Charcot–Marie–Tooth disease type 2A caused by mutation in a microtubule motor KIF1Bbeta. Cell 2001; 105: 587–97.

Received May 2, 2002. Revised July 29, 2002.
Accepted July 29, 2002

Acta Neuropathol (2003) 105 : 341–350
DOI 10.1007/s00401-002-0651-4

REGULAR PAPER

Nozomi Hishikawa · Yoshio Hashizume · Mari Yoshida
Gen Sobue

Clinical and neuropathological correlates of Lewy body disease

Received: 21 August 2002 / Revised: 22 October 2002 / Accepted: 22 October 2002 / Published online: 14 January 2003

Abstract We investigated distribution of neuronal and glial inclusions in 30 brains obtained at autopsy from patients with Lewy bodies (LBs) disease, which was clinically diagnosed as Parkinson's disease (PD), dementia with Lewy bodies (DLB), or pure autonomic failure (PAF). The cases were classified, according to the guidelines for the pathological diagnosis of DLB, into three types: the neocortical type, the limbic type, and the brain stem-predominant type. All postmortem brains had coil-like glial inclusions as well as LBs, and the distribution pattern and density of glial inclusions and LBs varied. The distribution of glial inclusions was strikingly similar to that of LBs. In the cerebral cortex in particular, the number of glial inclusions was fairly well correlated with the number of LBs, irrespective of the three pathological types. In the brain stem, distribution was similar between glial inclusions and LBs, and there was no distinct pathological difference among the three types. Glial inclusions and LBs were immunohistopathologically similar with respect to ubiquitin, α-synuclein, and Gallyas-Braak staining. The clinical features of the three types of LB disease were also similar; i.e., parkinsonism, some dementia, and/or autonomic failure. The inclusions in neurons and glial cells occurred in parallel with respect to tissue distribution and immunohistochemical features, suggesting that accumulation of neuronal and glial inclusions in the LB diseases have a common pathological feature. Our findings suggest that DLB, PD with and without dementia, and PAF share one clinicopathological entity.

N. Hishikawa · G. Sobue (✉)
Department of Neurology,
Nagoya University Graduate School of Medicine,
65 Tsurumai-cho, Showa-ku, 466–8550 Nagoya, Japan
Tel.: +81-52-7442385, Fax: +81-52-7442384,
e-mail: sobueg@med.nagoya-u.ac.jp

Y. Hashizume · M. Yoshida
Institute for Medical Science of Aging, Aichi Medical University,
Nagakute-cho, 480–1195 Aichi-gun, Japan

Keywords Parkinson's disease · Dementia with Lewy body disease · Pure autonomic failure · Lewy body · α-synuclein

Introduction

It is becoming increasingly evident that there is some overlap in the clinical and neuropathological features of Parkinson's disease (PD) with and without dementia, dementia with Lewy bodies (DLB), and pure autonomic failure (PAF) [2, 3, 4, 6, 14, 16, 20, 29]. Clinically, PD and DLB patients show parkinsonism and can show autonomic failure. DLB patients and some PD patients are demented. Pathologically, PD, DLB, and PAF patients share loss of pigmented neurons, usually evident among the pigmented and catecholaminergic neurons in the brain stem [8, 9, 11, 17, 21, 25], and the presence of Lewy bodies (LBs), which are intracytoplasmic, spherical, eosinophilic, α-synuclein-positive neuronal inclusions. Spongiform changes (microvacuolation) or LB-related neurites are often found in the temporal cortex of PD as well as DLB patients [7, 10, 15].

Recent studies showed that argyrophilic coil-like glial inclusions appear in the brain of PD and DLB patients, and that these inclusions are characterized by α-synuclein immunoreactivity, but not tau-protein immunoreactivity, and are present in both oligodendroglia and astrocytes [2, 12, 27, 31, 32, 33]. More recently, argyrophilic astrocytic star-like inclusions were reported in the cortex of DLB patients; these resembled tuft-shaped astrocytic fibrillary tangles, and were immunohistochemically negative for ubiquitin and α-synuclein [28]. These findings strongly suggest that glial cells are involved in the pathogenesis of both PD and DLB.

In the present study, we investigated the distribution of argyrophilic coil-like glial inclusions in relation to the presence of LBs and we examined spongiform change in autopsied brains of LB disease patients. We further assessed relation between the distribution patterns of neuronal and glial inclusions and clinical features.

Materials and methods

Subjects

We examined autopsy brains from 30 patients in whom the appearance of LBs was the main histopathological finding. The clinical characteristics of the 30 patients are shown in Table 1. The distribution and frequency of LBs were evaluated according to the consensus criteria for pathological diagnosis of DLB [22]. The number of LBs was counted in the brain regions [Brodmann area; BA8/9 (frontal), BA21 (temporal), BA24 (anterior cingulate), BA29 (transentorhinal), BA40 (parietal)] determined in the protocol (ubiquitin immunostain) and each region was given a score: 0 (no LBs), 1 (1–4 LBs), and 2 (≧5 LBs). The cases were then classified into three types, neocortical (n =8, patients age at death 65–84 years, mean 74.1 years), limbic (n =19, patients age at death 57–86 years, mean 75.4 years), and brain stem-predominant (n =3, patients age at death 60–71 years, mean 66.7 years), depending upon which area in each case was given total score. Disease duration for the neocortical type (cases 1–8) ranged from 4 to 13 years (mean 8.1 years), for the limbic type (cases 9–27) from 1 to 26 years (mean 9.9 years), and for the brain stem-predominant type (cases 28–30) from 8 to 21 years (mean 14.5 years). The presence of neurofibrillary tangles (NFTs) and senile plaques (SPs) were classified in each case according to the stages of Alzheimer's disease (NFT; I–IV, SP; A–C) as described by Braak and Braak [5] and CERAD [23]. No cases were included in our study that were given an NFT classification of III or IV or SPs classification of B or C, and other tau pathology, e.g., progressive supranuclear palsy, corticobasal degeneration, Pick's disease, and argyrophilic grain disease.

The medical records of the 30 patients were reviewed. Parkinsonism was considered present if there was any mention of resting tremor, rigidity, or akinesia. Dementia was noted as progressive cognitive decline, fluctuating cognition, memory disturbance, or impaired visuospatial performance. Autonomic failure was noted

Table 1 Clinical features of 30 cases of LB disease classified into three types: neocortical, limbic and brain stem predominant (*LB* Lewya body, *PD* Parkinson's disease, *PD+D* Parkinson's disease with dementia, *DLB* dementia with Lewy body, *PAF* pure autonomic failure, *SDS* Shy-Drager syndrome, *DIC* disseminated intravascular coagulation, *NA* not available, –absence, +presence)

Case	Age (years)	Sex	Duration (years)	Parkinsonism	Dementia	Duration of dementia (years)	Autonomic failure	Initial symptoms	Clinical diagnosis	Cause of death
Neocortical type										
1	70	F	13	+	+	1	NA	Tremor	PD+D	Pneumonia
2	70	M	7	+	+	6.5	+	NA	SDS	NA
3	65	M	5	+	+	2	+	Bradykinesia	DLB	NA
4	78	M	6	+	+	6	+	Bradykinesia	DLB	Pneumonia
5	77	M	11	+	+	6	+	Bradykinesia	SDS	Sepsis
6	77	M	12	+	+	12	NA	Tremor	PD+D	Sepsis
7	84	M	7	+	+	7	+	Bradykinesia	DLB	Respiratory insufficiency
8	72	M	4	+	+	1	+	Tremor	PD+D	Pneumonia
Limbic type										
9	73	M	26	+	+	4	–	Bradykinesia	PD+D	Pneumonia
10	81	M	14	+	+	2	–	Dysbasia	PD+D	Pneumonia
11	75	F	13	+	+	4	–	Tremor	PD+D	Pneumonia
12	84	M	11	+	+	7	+	Tremor	PD+D or DLB	Ileus
13	86	M	11	+	+	4	–	Dysbasia	PD+D	Respiratory insufficiency
14	80	M	5	+	+	2	+	Bradykinesia	PD+D or DLB	Pneumonia
15	71	M	8	+	+	3	+	Orthostatic hypotension	PD+D or DLB	Pneumonia
16	67	M	2.5	+	+	0.5	+	Orthostatic hypotension	PD+D or DLB	DIC
17	79	M	13	+	+	5	–	Tremor+dysbasia	PD+D or DLB	Pneumonia
18	69	M	1.1	+	–	–	+	Tremor+orthostatic hypotension	SDS	Sudden death
19	83	M	6	+	–	–	+	Tremor+dysbasia	PD	Pneumonia
20	80	M	17	+	–	–	+	Tremor	PD	Pneumonia
21	74	M	14	+	+	2	–	Dysbasia	PD+D	Hepatic insufficiency
22	75	M	?	+	+	4	+	NA	PD+D or DLB	Sudden death
23	71	M	12	+	–	–	–	Bradykinesia	PD	Sudden death
24	74	M	6	+	+	2	+	Tremor+dysbasia	PD+D or DLB	Sudden death
25	81	M	?	+	NA	NA	NA	NA	PD	Sudden death
26	57	M	1.6	+	–	–	NA	Bradykinesia	PD	Pneumonia
27	72	M	4	+	NA	NA	NA	NA	PD	Pneumonia
Brain stem-predominant type										
28	69	F	21	+	–	–	+	Tremor	PD	Sudden death
29	60	M	8	–	–	–	+	Lethargy	PAF or SDS	Sudden death
30	71	M	NA	–	–	–	+	NA	PAF	Sudden death

if there was mention of signs of orthostatic hypotension, such as postural faintness, blurred vision, syncope, or a drop in blood pressure (>30 mmHg in systolic pressure) in response to upright posture. Head-up tilt test and metaiodobenzylguanidine myocardial scintigraphy findings were also noted.

Histopathology and immunocytochemistry

All brains were removed within 12 h of death and immersed in 20% neutral-buffered formalin. Brain areas were sliced into 5-mm-thick sections along various planes: frontal plane for the cerebrum, horizontal plane for brain stem and spinal cord, and sagittal plane for cerebellum. The tissues were embedded in paraffin and sectioned at 8-μm thickness. For routine histological examination, each section was stained with hematoxylin and eosin (H-E) and Klüver-Barrera (K-B) stains. Selected sections were also stained with the Bodian and Holzer stains. In all cases, additional sections taken from the cerebrum, brain stem, cerebellum and spinal cord were stained by the Gallyas-Braak (G-B) method and immunostained by the avidin-biotin-peroxidase complex method. The following antibodies were used: anti-α-synuclein (polyclonal, at 1:400; Santa Cruz Biotech., Calif.); anti-ubiquitin (polyclonal, at 1:600; DAKO, Glostrup, Denmark); anti-tau (TAU-2, monoclonal, at 1:500; Sigma, St. Louis, Mo.); anti-paired helical filament (PHF)-tau (AT-8, monoclonal, at 1:1,000; Innogenetics, Ghent, Belgium). For staining with anti-α-synuclein antibody, the sections were pretreated with 99% formic acid (Wako, Osaka, Japan) for 5 min at room temperature.

For electron microscopy, selected light microscopy sections staining with anti-α-synuclein were reused. They were washed in phosphate buffer, postfixed with 1% osmium tetroxide, dehydrated in a graded series of ethanol and embedded in Epon. The sections were cut into 65 nm, and examined with an electron microscope at 75 kV (Hitachi H-7000, Tokyo, Japan).

Quantification of LBs and coil-like glial inclusions

Frequency and distribution of the LBs were assessed by ubiquitin staining according to the guidelines for the pathological diagnosis of dementia with LBs [22]. Following these guidelines, the number of ubiquitin-positive LBs was counted in the brain regions determined in the protocol, including frontal, temporal, parietal, anterior cingulate, and transentorhinal, and converted into scores from 0 to 2.

Argyrophilic coil-like glial inclusions were counted in the same regions of cerebral cortex in which LBs were assessed. The midbrain was cut at the level of the superior colliculus and oculomotor nucleus; the pons was cut at the level at which the locus ceruleus was the most extended, and the medulla was cut at the level of the dorsal vagal nucleus through the middle of the inferior olivary nucleus. The glial inclusions were counted in each area (1.5×1.5 mm^2×10 fields) of the substantia nigra, tegmentum of the pons, and tegmentum of medulla (Fig. 1). The areas were given a score, depending upon the numbers of inclusions found; 0, none; +, 1–50/22.5 mm^2; ++, 51–100/22.5 mm^2; +++, 101–200/22.5 mm^2; and ++++, >200/22.5 mm^2.

The correlations between the number of glial inclusions and LBs in the cingulated gyrus and in the transentorhinal cortex were studied. Spearman's linear correlation analysis was used to determine any relationship between them. Statistical analysis was performed with the statistical package StatView (Abacus Concepts Inc., Berkeley, Calif.).

Results

Distribution of LBs and coil-like glial inclusions

Neocortical type

In all neocortical cases, a number of LBs were found in the residual neurons of the substantia nigra, locus ceruleus, dorsal vagal nucleus, and intermediate lateral nucleus of the spinal cord, in the hypothalamus, Meynert's nucleus, and amygdala, as well as in cerebral cortex (Figs. 2A, 3A,B). In each of the five areas of the cerebral cortex, LBs were found more frequently than those of the limbic and brain stem-predominant types; the LB scores were 7–10. In the limbic area, LBs were detected frequently in the anterior cingulate BA24, and transentorhinal BA29 (Table 2).

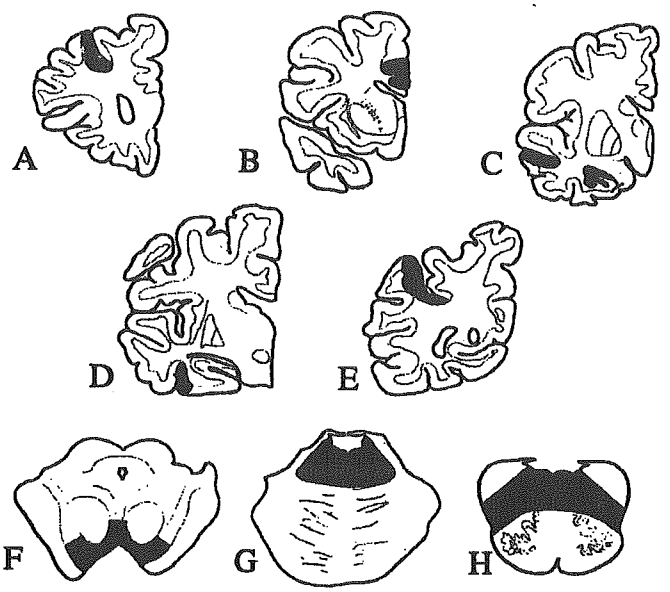

Fig. 1 A–E Five areas of the cerebral cortex were sampled for evaluation of the number of Lewy body and glial inclusion are shown. These areas were defined according to the guideline for evaluation of LB distribution and pathological diagnosis of dementia with LBs. F–H In the dorsomedial part of the substantia nigra, tegmentum of the pons, and tegmentum of the medulla, the coil-like glial inclusions were counted in ten 1.5×1.5 mm^2 fields. Glial inclusions were found more frequently in these areas (*LB* Lewy body)

Argyrophilic coil-like inclusions were distributed widely in the central nervous system (Figs. 2B, 3D), the brain stem (midbrain, pons, medulla), cerebral cortex, cerebral white matter, striatum, globus pallidus, thalamus, hypothalamus, amygdala, Meynert's nucleus, accumbens, olfactory tubercle, hippocampus, intralaminar nucleus of thalamus, cerebellum (white matter, superior and inferior cerebellar peduncle), and the spinal cord (especially the lateral and anterior horn and the lateral anterior funiculus). The distribution patterns were similar to these of the LBs (Fig. 2A, B). The glial inclusions were immunoreactive for α-synuclein and ubiquitin (Fig. 3E–H) but not for tau or PHF-tau protein. Immunoelectron microscopically, the glial inclusions consisted of filamentous structures approximately 25–45 nm in diameter, and associated granular structures (Fig. 3I, J).

Limbic type

The number of LBs in the cerebral cortex in the limbic type cases represents a transition between neocortical type

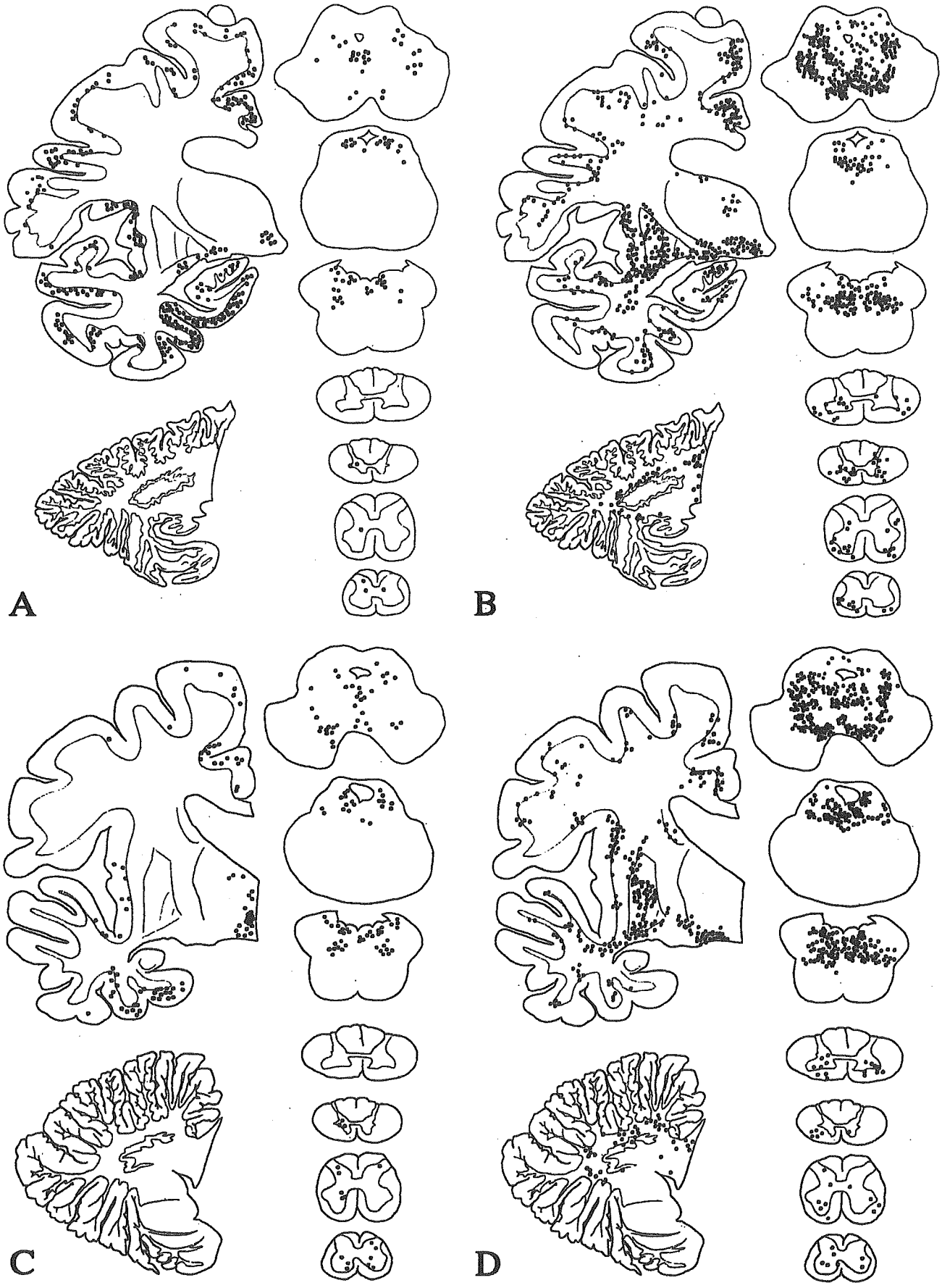
A
B
C
D

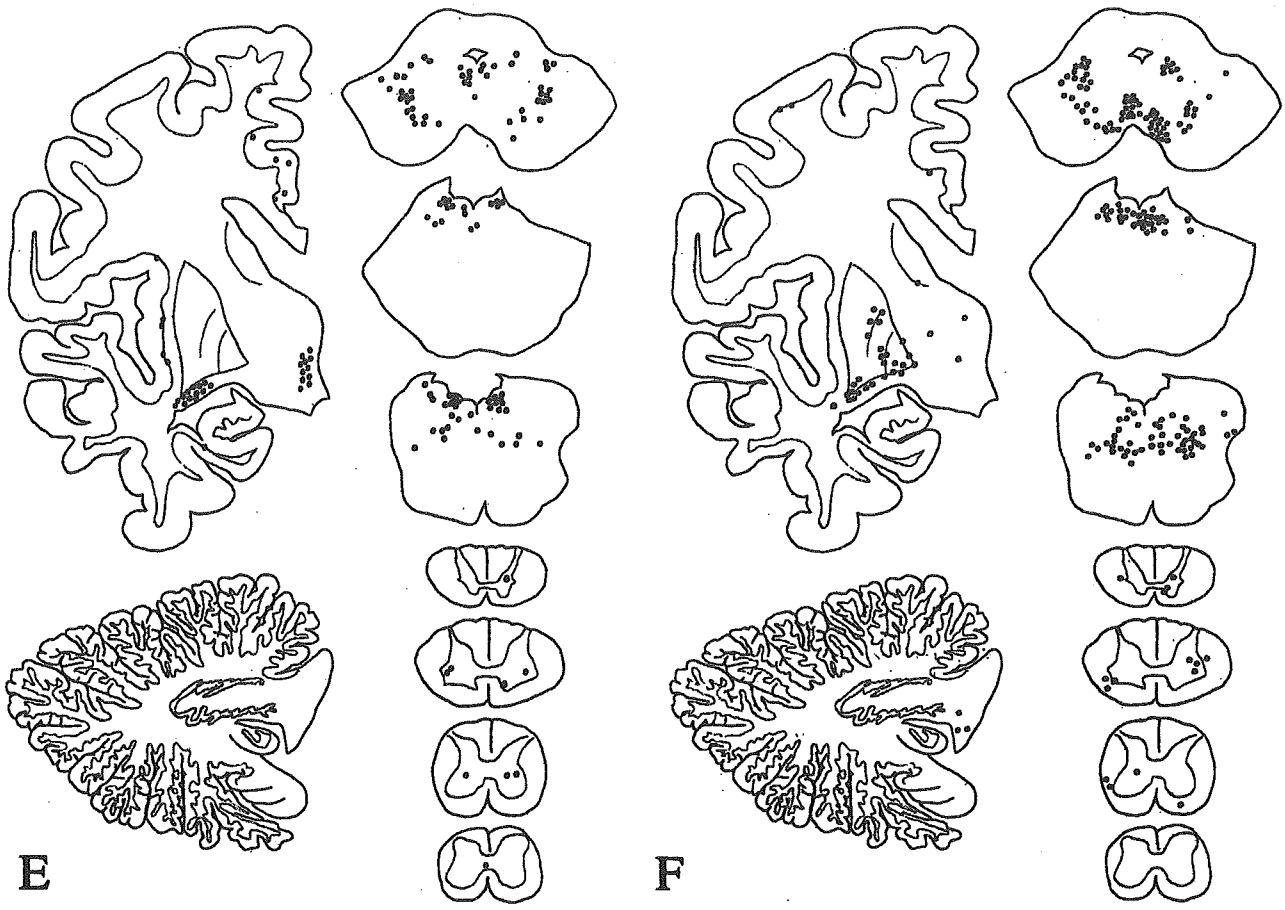

Fig. 2 Distribution of LBs and argyrophilic coil-like inclusions. In each sections LBs and glial inclusions are plotted; each dot represents one ubiquitin-immunoreactive LB or argyrophilic glial inclusion. A, B Neocortical type, C, D limbic type; E, F brain stem-predominant type. A, C, E LBs stained with ubiquitin immunocytochemistry; B, D, F argyrophilic coil-like glial inclusions

and brain stem predominant type. LBs were distributed in the cerebral cortex (especially the anterior cingulate and transentorhinal cortex), hypothalamus, Meynert's nucleus, amygdala, brain stem nucleus, spinal cord, and the LB scores ranged from 3 to 6 (Fig. 2C). Argyrophilic coil-like inclusions were widely dispersed (Fig. 2D), and the distribution pattern was similar to that of the LBs (Fig. 2C, D).

Brain stem-predominant type

In this study, only three cases belonged to this type. Numerous LBs appeared in the brain stem nucleus of substantia nigra, locus ceruleus, dorsal vagal nucleus, intermediate lateral nucleus of the spinal cord, hypothalamus, Meynert's nucleus, and amygdala. Within the cerebral cortex, only a few LBs were detected, and these were mainly in the limbic area (Fig. 2E), and LB scores were 2.

The argyrophilic glial inclusions in this group were distributed mainly in the brain stem and spinal cord (lateral and anterior horn and the lateral anterior funiculus). A small number of glial inclusions were seen in the cerebral cortex, hypothalamus, striatum, globus pallidus Meynert's nucleus, amygdala, and cerebellum (Fig. 2F). The LBs and argyrophilic glial inclusions distribution patterns were similar in all three cases.

Common features

The distribution and density of argyrophilic glial inclusions and Lewy bodies in the cases overall are shown in Table 2. The distribution and density of glial inclusions in the brain stem did not differ between pathological types. Within the cerebral cortex, the number of coil-like glial inclusions in each area was fairly well correlated with the number of LB (Fig. 4A, B). Both LBs and glial inclusions were found most frequently in the limbic area of the cerebral cortex.

Neuritic degeneration demonstrable by immunostaining for α-synuclein and ubiquitin occurred in substantia nigra, dorsal vagal nucleus, Meynert's nucleus, amygdala, CA2/3 region of the hippocampus and other regions (Fig. 3C). The change in the CA2/3 region was found more frequently in the neocortical and limbic type cases.

Table 2 Neuropathological findings in 30 cases with LB disease classified into three types. For criteria for semiquantification see text: *A*, *B*; stages of SP by Braak and Braak; I and II stage of NFT by Braak and Braak (*NFT* neurofibrillary tangle, *SP* senile plaque, *SN* substantia nigra, *P* tegmentum of pons, *IMR* intermediate reticular zone, *GI* glial inclusion, *LB* Lewy body, *NA* not available, *N* not done, –absent, +very mild, ++mild, +++moderate, ++++severe,)

Case	Brain weight (g)	NFT	SP	Spongiform change	Coil-like GI			Coil-like GI count/area						LB count/area					
					SN	P	IMR	Transentorhinal	Cingulate	Temporal	Frontal	Parietal	Total	Transentorhinal	Cingulate	Temporal	Frontal	Parietal	Total (LB score)
Neocortical type																			
1	1,140	I	–	–	+++	+	+	32	35	5	20	6	98	37	117	17	10	16	197 (10)
2	1,340	I	–	++	++++	+++	++++	13	11	4	2	6	36	92	38	16	3	6	155 (9)
3	1,240	I	–	+++	+++	+	++	7	10	10	1	2	30	10	26	5	1	7	49 (9)
4	1,070	I	A	++	+++	+	+	6	15	2	6	1	30	30	28	8	4	1	71 (8)
5	1,100	I	A	+++	+	+	+++	17	8	3	1	0	29	117	56	25	1	15	214 (9)
6	1,210	I	–	++	++++	+++	++++	5	15	1	2	0	23	25	51	6	2	0	84 (7)
7	1,170	I	B	+++	++++	+++	++	5	4	1	1	2	13	31	25	8	4	5	73 (9)
8	1,400	II	A	+	++	+	++	2	3	0	2	0	7	11	40	38	6	2	97 (9)
Limbic type																			
9	1,260	I	–	++	++++	++	++	3	46	0	3	0	52	14	56	3	2	0	75 (6)
10	1,230	I	–	–	++++	+++	+++	10	27	5	4	3	49	13	11	0	1	1	26 (6)
11	1,300	I	A	+	++++	++	++	25	19	1	0	1	46	22	26	2	1	0	51 (6)
12	1,160	I	A	++	+++	++	++	12	16	3	0	0	31	17	37	4	3	0	61 (6)
13	1,040	I	–	–	++++	+++	+++	1	15	0	4	0	20	12	16	3	0	0	31 (5)
14	1,440	I	B	–	++++	++	++	2	10	1	3	3	19	8	37	3	2	0	50 (6)
15	1,040	I	A	–	+++	+++	++++	5	9	1	0	0	15	10	7	1	1	0	19 (6)
16	1,260	I	–	–	+++	+	+	2	7	1	2	1	13	15	19	1	1	0	36 (6)
17	1,170	II	A	++	+++	+++	++++	2	7	1	1	0	11	7	28	1	0	0	36 (6)
18	1,530	I	–	–	+	++	++	11	0	0	0	0	11	5	7	0	0	0	12 (4)
19	1,120	I	–	–	+	+	+	2	2	0	1	2	7	10	5	2	0	0	17 (5)
20	1,509	I	–	–	++++	++	+++	2	4	0	0	0	6	10	3	0	0	0	13 (3)
21	1,220	I	–	–	++++	+	++	2	2	0	1	0	5	7	4	0	4	0	15 (4)
22	1,400	I	–	–	+++	++	++	0	3	0	1	0	4	0	5	1	0	1	7 (4)
23	NA	I	–	–	+++	+	++	2	0	0	0	0	2	3	5	0	0	0	8 (3)
24	1,210	–	–	–	++	+	+	0	0	0	0	0	0	3	7	0	0	0	10 (3)
25	NA	I	–	–	+	+	+	2	1	0	0	N	N	2	3	1	0	0	6 (3)
26	NA	I	–	–	N	N	N	0	2	0	1	N	N	2	2	2	1	N	N
27	1,300	–	–	–	+++	+++	+++	N	N	N	N	N	N	14	13	0	0	0	27 (4)
Brainstem-predominant type																			
28	1,200	II	A	–	+++	+	+	1	3	2	3	2	11	1	1	0	0	0	2 (2)
29	1,250	–	–	+	+	+	+	0	0	0	0	0	0	1	1	0	0	0	2 (2)
30	NA	I	A	–	+	+	++	0	1	0	0	0	1	2	3	0	0	0	5 (2)

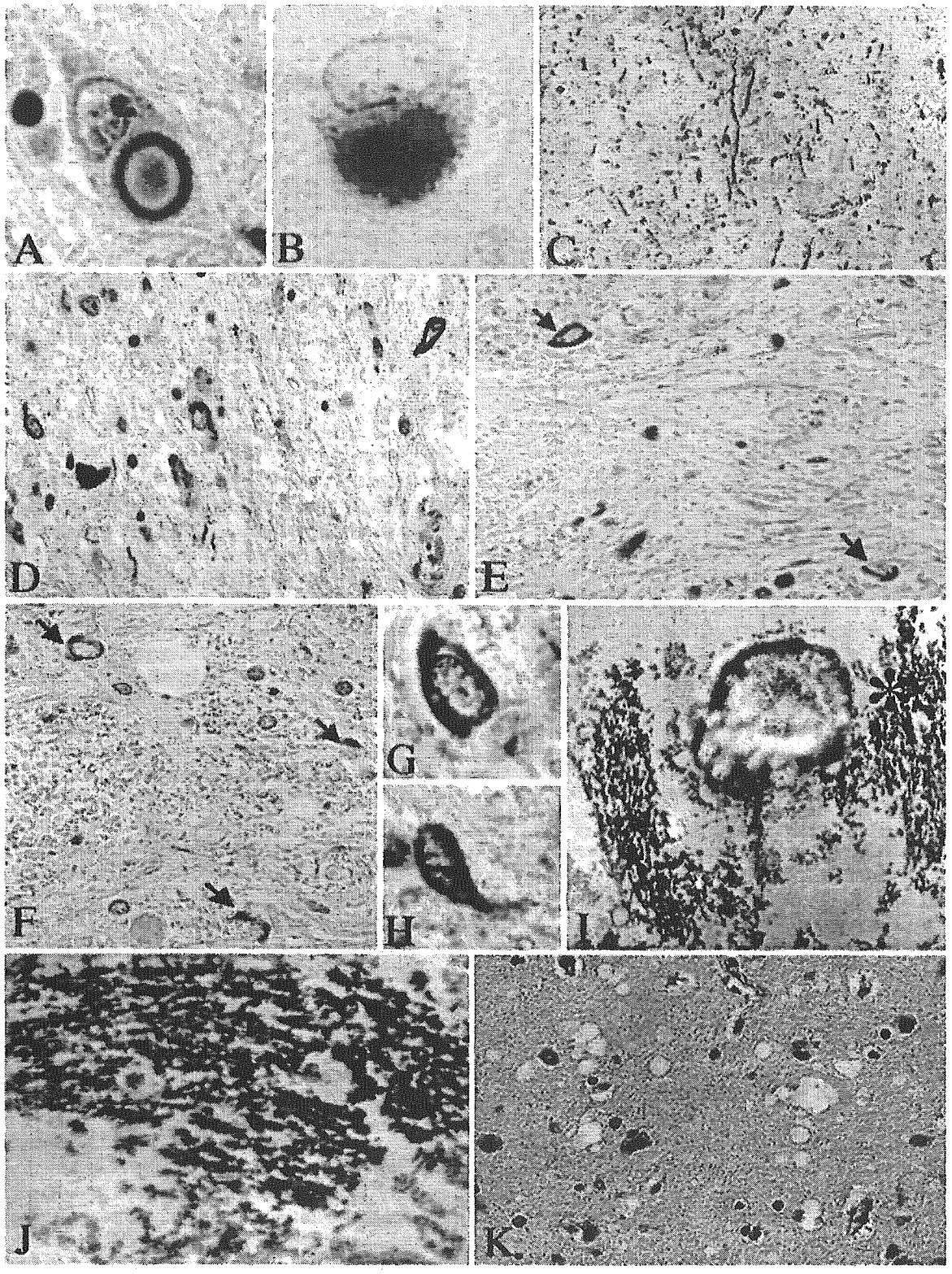

Fig. 3 A α-Synuclein-positive brain stem-type LB. B Ubiquitin positive cortical LB, which is also immunostained by anti-α-synuclein antibody. C In the CA2-3 sector of the hippocampus, numerous neuritic changes can be observed by α-synuclein immunostaining. D Coil-like inclusions in the substantia nigra. E Ubiquitin-positive glial inclusion in the medulla. F α-Synuclein-positive glial inclusion in the medulla. G Higher magnification of the ubiquitin-positive glial inclusion in the medulla. H Higher magnification of the α-synuclein-positive glial inclusion in the medulla. I Immunoelectron micrograph of α-synuclein-positive glial inclusion in putamen. J High-power view of the glial inclusion (*asterisk*) in I. K Spongiform changes within the temporal neocortex. A, C, F, H–J α-Synuclein immunostaining; B, E, G ubiquitin immunostaining; D Gallyas-Braak stain; K hematoxylin-eosin. A ×1,000; B ×900; C, K ×200; D–F ×400; G, H ×1,500; I ×8,000; J ×20,000

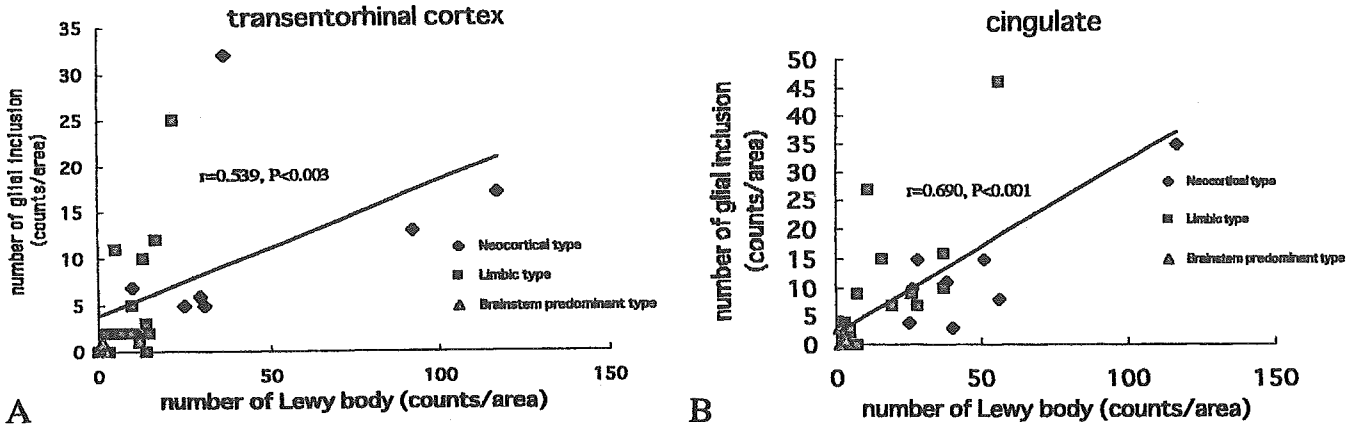

Fig. 4 Correlation of the total number of glial inclusions and LBs in the transentorhinal cortex (A) and anterior cingulated gyrus (B). Total inclusions counts correlate well to the total counts of LBs (transentorhinal cortex; r =0.539, P <0.003, and anterior cingulated gyrus; r =0.690, P <0.001). The areas of the transentorhinal cortex and anterior cingulated gyrus were defined according to [22]

Spongiform changes (microvacuolation)

Spongiform changes were found most frequently in the neocortical-type cases and were found only occasionally in the other two types of cases (Table 2) (Fig. 3K). Spongiform changes were largely restricted to the temporal neocortex, amygdale, and cingulate gyrus.

Clinical and pathological correlation

In this study, all neocortical type cases involved parkinsonism and dementia, and autonomic failure was noted in all cases examined. Dementia appeared within 1 year of the onset of parkinsonism in cases 2, 4, 6, and 7. Cases 1, 3, 5, and 8 also showed dementia, but this appeared more than 1 year after the onset of parkinsonism. Clinical diagnosis was DLB in 3 cases, PD with dementia in 3 cases, and Shy-Drager syndrome in 2 cases (Table 1).

All limbic type cases involved parkinsonism (Table 1). Twelve of 17 patients (70.6%) who were examined were demented. Severe and fluctuating cognition, and impairment of visuospatial performance were observed in 4 of these 12 cases (cases 15, 17, 21, 24). In all cases, the onset of dementia was more than 1 year after the appearance of parkinsonism. There was no sign of dementia in 7 cases, and, in 9 of 16 patients (56.2%) who could be examined, autonomic failure was seen. The clinical diagnosis was PD with dementia in 12 cases, PD in 6, and Shy-Drager syndrome in 1.

All of the brain stem-predominant type cases involved symptom of autonomic failure. There was only one case that involved parkinsonism that carried a diagnosis of PD. Two other cases that had no sign of parkinsonism carried a diagnosis of PAF. Dementia was not noted in any of the brain stem-type cases (Table 1).

Discussion

Theappearance of LBs is a common neuropathological feature and a principal hallmark of both PD and DLB; LBs are also found in PAF [11]. LBs are eosinophilic neuronal inclusion bodies, with α-synuclein being a major component [14, 28]. There have been several resent studies showing that cytoplasmic aggregation of α-synuclein also occurs in glial cells in the brains of both PD and DLB patients [2, 12, 32, 33]. These inclusions can be distinguished from glial fibrillary tangles, glial cytoplasmic inclusions, and coiled bodies by their distribution pattern, shape, α-synuclein positivity, tau protein negativity, and presence in both oligodendroglia and astrocytes. However, the frequency and precise distribution of such glial inclusions and their relation to the presence of LBs have not yet been clarified. Thus, we investigated the relation between the distribution pattern of α-synuclein aggregates in neurons and glial cells and the clinical phenotypes.

We confirmed that aggregation of α-synuclein occurred in both neurons and glial cells in all cases of LB disease. The pattern of LBs distribution in the cerebral cortex differed among the three pathological types. The distribution pattern in the brain stem and spinal cord, however, was quite similar among the three types. All 30 cases showed abundant coil-like glial inclusions to various degrees, and these were distributed extensively in the cerebral cortex, white matter of the cerebrum and cerebellum and the spinal cord, and most frequently in the brain stem. In our study, we used 8-μm-thick sections for G-B staining and immunocytochemistry, and performed formic acid pretreatment, which markedly enhanced α-synuclein immunoreactivity. This treatment is suggested to enhance the glial inclusions, and in the present study these were found to be more widespread than has been reported previously.

In any given individual, the distributions of LBs and coil-like glial inclusions were similar in the brain stem and cerebral cortex independent of types of pathological classification. The underlying pathological basis for this parallel distribution of LBs and glial inclusions is unknown, but we can speculate that glial inclusions are related pathogenically to the process of LB formation. Abeliovich et al. [1] recently reported that α-synuclein-defi-